International Journal of Innovative
Computing, Information and Control
Volume **9**, Number **4**, April **2013**

 ISSN 1349-4198
pp. **1539–1556**

A NEW CONCEPT ON PI DESIGN FOR TIME DELAY SYSTEMS: WEIGHTED GEOMETRICAL CENTER

Cem Onat

Department of Mechanical Engineering
Faculty of Engineering
Inonu University
44280, Malatya, Turkey
cem.onat@inonu.edu.tr

Received February 2012; revised June 2012

Abstract. *In this paper, a new concept on PI design for time delay systems is introduced. The concept is weighted geometrical center of the stabilizing controller parameters region. Calculating of the stabilizing control parameters region is based on plotting the stability boundary locus in the (k_p, k_i) plane and then computing stabilizing values of the parameters of a PI controller. The weighted geometrical center point of this region is computed by using coordinates of the boundary points. In the simulations, stabilizing controllers in a trial circular area centered at the weighted geometrical center point are studied. Simulation results show that the weighted geometrical center point is a special point in terms of compromising on the transient state characteristics.*
Keywords: PI controller, Design method, Weighted geometrical center

1. **Introduction.** In system modeling and control, the existence of a time delay in input-output relations is an important consideration [1,2]. It is well known that time delays as a source of the generation of oscillation and a source of instability are frequently encountered in various engineering systems such as long transmission lines in pneumatic systems, nuclear reactors, rolling mills, hydraulic systems, engines and manufacturing processes. Many studies have concluded that time delay will reduce the phase margin of control systems and yield reduced relative stability. Thus, the presence of such time delay will greatly increase the difficulty of achieving satisfactory performance. For reviews of recent results on time delay systems, see [3].

Although several advanced control strategies have been developed, structurally simple proportional-integral (PI), proportional-integral-derivative (PID) and lag/lead controllers are still widely used in industrial control systems because of their robust performance and simplicity. Therefore, the subject of the designing PI, PID and lag/lead controllers is of great importance for researchers. Several methods for determining parameters of these controllers have been developed during the past sixty years [4-6]. Some of the most popular methods are the Ziegler-Nichols tuning method, the Astrom-Hagglund auto tuning method and other methods based on integral performance criteria. However, many important results have been recently reported on computation of all stabilizing P, PI and PID controllers after the publication of work by Ho et al. [7-10]. A new and complete analytical solution which is based on the generalized version of the Hermite-Biehler theorem has been provided in [7] for computation of all stabilizing constant gain controllers for a given plant. A linear programming characterization of all stabilizing PI and PID controllers for a given plant has been obtained in [8,10]. This characterization besides being computationally efficient has revealed important structural properties of PI and

PID controllers. For example, it was shown that for a fixed proportional gain, the set of stabilizing integral and derivative gains lies in a convex set. This method is very important since it can cope with systems that are open loop stable or unstable, minimum or nonminimum phase. However, the computation time for this approach increases in an exponential manner with the order of the system being considered. It also needs sweeping over the proportional gain to find all stabilizing PI and PID controllers which is a disadvantage of the method. An alternative fast approach to this problem based on the use of the Nyquist plot has been given in [11,12]. An extension of the method given in [11] to the lad-lead controller structure has been given in [13]. A parameter space approach using the singular frequency concept has been given in [14] for design of robust PID controllers. More direct graphical approaches to this problem based on frequency response plots have been given in [15,16]. The major problem for this approach is the requirement for frequency gridding. In [17], a method has been given for computation of stabilizing PI controllers in the parameter plane, (k_p, k_i)-plane. In this method, the result of [12] has been used to avoid the problem of frequency gridding. Thus, a very fast way of calculating the stabilizing values of PI controllers for a given control system has been obtained. Recently, a graphical method to compute all feasible gain and phase margin specifications-oriented PID controllers based on this method has been reported in [18] where, it has considered both parametric uncertainty and varying time delay. As a result of this study, Kharitonov region is proposed for robust PID controllers for uncertain systems with time varying delay. None of above mentioned methods have dealt with numerically tuning of PI and PID controller parameters. A common trait of these methods leads to calculating the stability region in the controller parameters space. However, the numbers of controllers in these regions are endless and it is not clear that which point can be selected.

In this paper, a new concept on PI tuning method based on stabilizing controller parameters region for the time delay systems is presented. The concept is weighted geometrical center of stabilizing controller parameters region. The region in the controller parameter space is computed by using the stability boundary locus method [17]. The weighted geometrical center point which can be used as a design preference is computed by means of the density of stability boundary points. The most important property of the method is its simplicity and reliability for determining the PI controller parameters according to the other PI tuning methods in the literature [5,19-21]. In practice, the method provides an algorithmic tool which has guaranteed stability and can be applied to other systems.

The paper is organized as follows. The next section summarizes the fundamental properties of the stability boundary locus technique. In Section 3, the derivation of the weighted geometric center for PI controller tuning is presented. Simulations are considered in Section 4 to illustrate the wisdom of the presented concept. Finally, concluding remarks are given in Section 5.

2. **Stability Region for a PI Controller.** In this section, a method is presented to obtain the stability region using the stability boundary locus approach [17]. Consider the single-input (r) single-output (y) (SISO) control system shown in Figure 1 where

$$G(s) = G_P(s) \cdot e^{-\theta s} = \frac{N(s)}{D(s)} \cdot e^{-\theta s} \tag{1}$$

is the plant to be controlled and $C(s)$ is the PI controller of the form

$$C(s) = k_p + \frac{k_i}{s}. \tag{2}$$

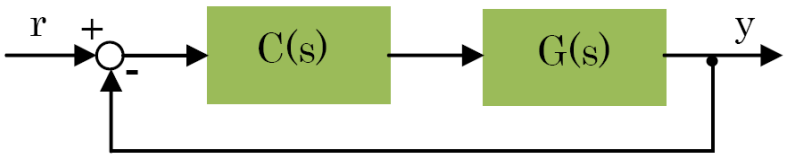

FIGURE 1. Block diagram of the control system

The problem is to find the stability region which includes all the parameters of the PI controller of (2) which stabilize the given system. The closed-loop characteristic polynomial $P(s)$ of the system, i.e., the numerator of $1 + C(s)G(s)$, can be written as

$$P(s) = s \cdot D(s) + (k_p \cdot s + k_i) \cdot N(s) \cdot e^{-\theta \cdot s}. \tag{3}$$

Decomposing the numerator and the denominator polynomials of $G_P(s)$ in (1) into their even and odd parts, and substituting $s = j\omega$, gives

$$G_P(\omega) = \frac{N_e(-\omega^2) + j \cdot \omega \cdot N_o(-\omega^2)}{D_e(-\omega^2) + j \cdot \omega \cdot D_o(-\omega^2)}. \tag{4}$$

For simplicity $(-\omega^2)$ will be dropped in the following equations. Thus, the closed-loop characteristic polynomial of (3) can be written as

$$P(\omega) = P_R(\omega) + j \cdot P_I(\omega) \tag{5}$$

where

$$P_R(\omega) = (k_i \cdot N_e - k_p \cdot \omega^2 \cdot N_o)\cos(\omega\theta) + \omega \cdot (k_i \cdot N_o + k_p \cdot N_e) \cdot \sin(\omega\theta) - \omega^2 \cdot D_o, \tag{6}$$

$$P_I(\omega) = -(k_i \cdot N_e - k_p \cdot \omega^2 \cdot N_o)\sin(\omega\theta) + \omega \cdot (k_i \cdot N_o + k_p \cdot N_e) \cdot \cos(\omega\theta) + \omega \cdot D_e. \tag{7}$$

Then, equating the real and imaginary parts of $P(\omega)$ to zero, two equations are obtained as

$$Q(\omega) \cdot k_p + R(\omega) \cdot k_i = X(\omega), \tag{8}$$

$$S(\omega) \cdot k_p + U(\omega) \cdot k_i = Y(\omega) \tag{9}$$

where

$$Q(\omega) = \omega \cdot N_e \cdot \sin(\omega\theta) - \omega^2 \cdot N_o \cdot \cos(\omega\theta), \tag{10}$$

$$S(\omega) = \omega \cdot N_e \cdot \cos(\omega\theta) + \omega^2 \cdot N_o \cdot \sin(\omega\theta), \tag{11}$$

$$R(\omega) = N_e \cdot \cos(\omega\theta) + \omega \cdot N_o \cdot \cos(\omega\theta), \tag{12}$$

$$U(\omega) = \omega \cdot N_o \cdot \cos(\omega\theta) - N_e \cdot \sin(\omega\theta), \tag{13}$$

$$X(\omega) = \omega^2 \cdot D_o, \tag{14}$$

$$Y(\omega) = -\omega \cdot D_e. \tag{15}$$

Finally, by solving the 2-dimensional system of (8)-(15) the parameters of PI controller are obtained as

$$k_p = \frac{(\omega^2 \cdot N_o \cdot D_o + N_e \cdot D_e) \cdot \cos(\omega \cdot \theta) + \omega \cdot (N_o \cdot D_e - N_e \cdot D_o) \cdot \sin(\omega \cdot \theta)}{-(N_e^2 + \omega^2 \cdot N_o^2)}, \tag{16}$$

$$k_i = \frac{-\omega \cdot (\omega^2 \cdot N_o \cdot D_o + N_e \cdot D_e) \cdot \sin(\omega \cdot \theta) + \omega^2 \cdot (N_o \cdot D_e - N_e \cdot D_o) \cdot \cos(\omega \cdot \theta)}{-(N_e^2 + \omega^2 \cdot N_o^2)}. \tag{17}$$

Changing ω from 0 to ∞, the stability boundary locus, $l(k_p, k_i, \omega)$ is constructed in the (k_p, k_i) plane using (16) and (17).

As a special case, a real root can cross over the imaginary axis at $s = 0$. Thus, a real root boundary is obtained by substituting $s = 0$ in $P(s)$ of (3). Therefore, this special boundary is determined as

$$k_i = 0. \tag{18}$$

The stability boundary locus and the real root boundary divide the parameter plane (k_p, k_i) into stable and unstable regions. The stable region can be obtained by choosing a test point within each region.

Example 2.1. *Consider the transfer function of the first order plus time delay (FOPTD) system has the form*

$$G(s) = \frac{N(s)}{D(s)} \cdot e^{-\theta s} = \frac{1}{s+1} e^{-0.5 \cdot s}. \tag{19}$$

Here, the aim is to obtain all stabilizing values of k_p and k_i that make the closed loop system in Figure 1 stable. The following equations are obtained after equating the real and imaginary part of characteristic to zero.

$$k_p \cdot \omega \cdot \cos(0.5 \cdot \omega) - k_i \cdot \sin(0.5 \cdot \omega) = \omega, \tag{20}$$

$$k_p \cdot \omega \cdot \sin(0.5 \cdot \omega) + k_i \cdot \cos(0.5 \cdot \omega) = -\omega^2 \tag{21}$$

The plotting of the stability boundary locus is executed by cooperative analyzing of Equations (20) and (21) for each value of ω. Hereunder, k_p, k_i pairs are obtained accordingly to ω values. Then, computed k_p, k_i pairs are figured in (k_p, k_i)-plane.

Figure 2 shows the stability boundary locus for a range of frequency (0, 10 rad/s) and the real root boundary line. It can be observed from this figure that the parameter plane is divided into four regions, namely R_1, R_2, R_3 and R_4. By choosing one arbitrary test point in each region, the stability region which is the shaded region (R_2) shown in Figure

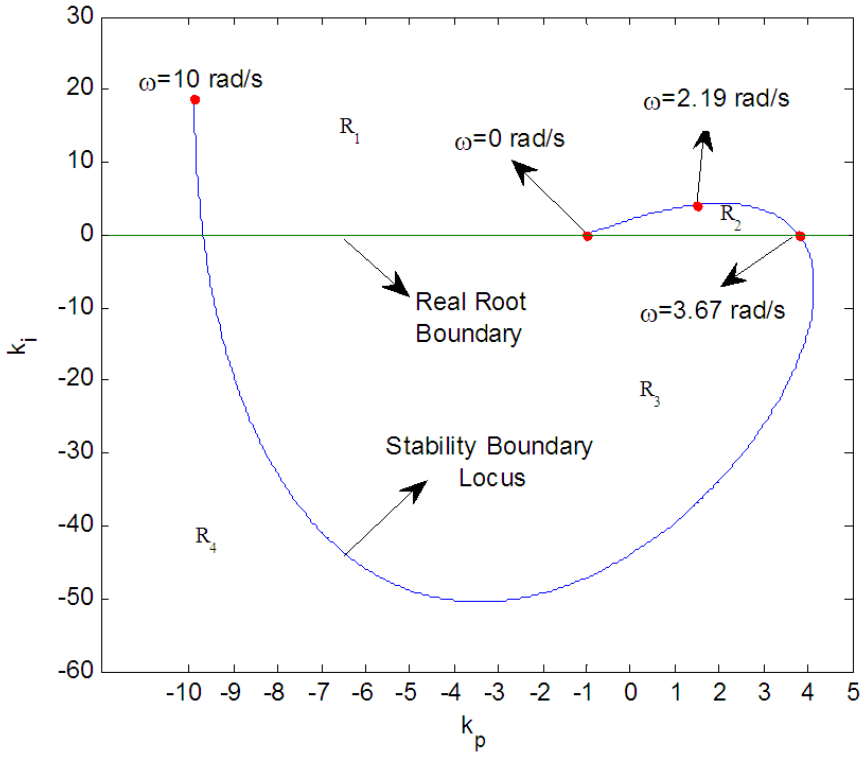

FIGURE 2. Stability boundaries of the FOPDT system

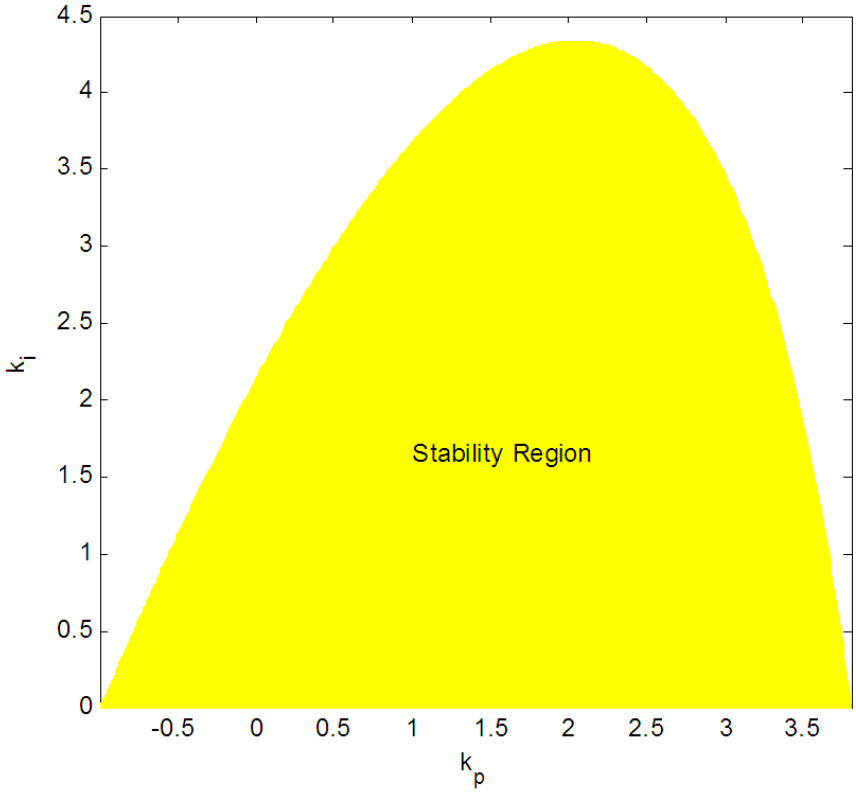

FIGURE 3. Stability region of the system

2 can be determined. Figure 3 shows more clearly R_2 for all stabilizing values of k_p and k_i. In this figure, the stability boundary locus is computed for the range of $\omega\,[0, \omega_i]$. The intersection frequency ω is calculated as 3.67 rad/s.

3. **Weighted Geometrical Center.** The points based stability boundary locus for the FOPTD system in (19) are shown in Figure 4. In this figure, each (k_p, k_i) points are marked by changing ω from 0 to 3.67 in steps of 0.01. It is seen from this figure that the distance between each points is not same. The points are closely spaced at small ω values. With growing the values of ω, they become distant and then tighten around the peak point of stability boundary locus and finally unwraps when reached the stability boundary locus to the real root boundary (k_p-axis).

This locus enclosing the stability region consists of n points of which the coordinates named are defined as (k_{p1}, k_{i1}), (k_{p2}, k_{i2}), (k_{p3}, k_{i3}), $\ldots$, (k_{pn}, k_{in}). For this example, n equals to 368.

Remark 3.1. *Note that the stability region is not closed form in the example. A part of stability region boundary consists of real root boundary (k_p-axis). Therefore, projections of boundary locus points on k_p-axis are considered for that stability region is obtained in closed form. The projections of the points in the stability boundary locus are shown in Figure 5. In this case, the coordinates of the projection points are $(k_{p1}, 0)$, $(k_{p2}, 0)$, $(k_{p3}, 0)$, $\ldots$, $(k_{pn}, 0)$.*

As a result of combining the points of stability boundary locus and real root boundary line, the weighted geometrical center (k_{pw}, k_{iw}) of the stability region is obtained easily

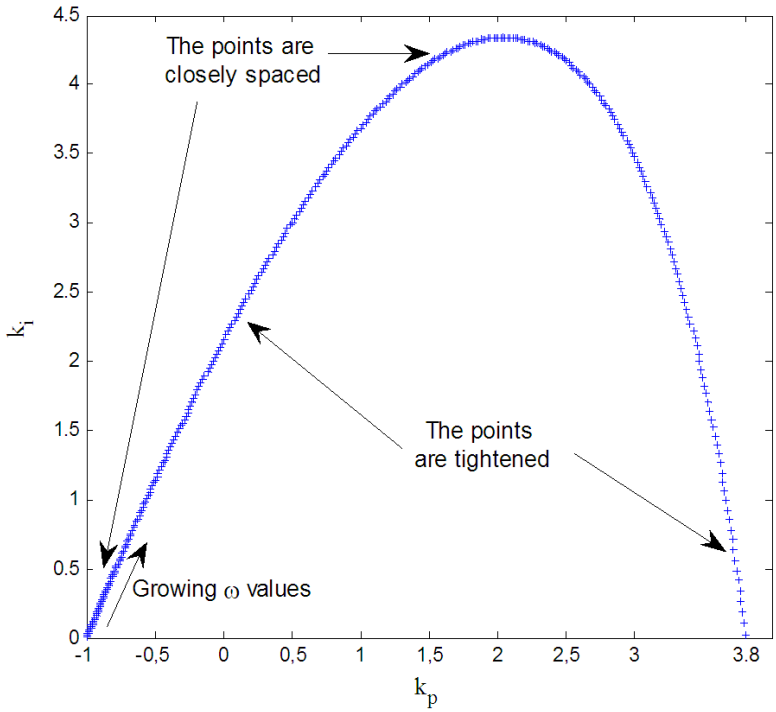

FIGURE 4. (k_p, k_i) points constituting the stability boundary locus depending on ω values

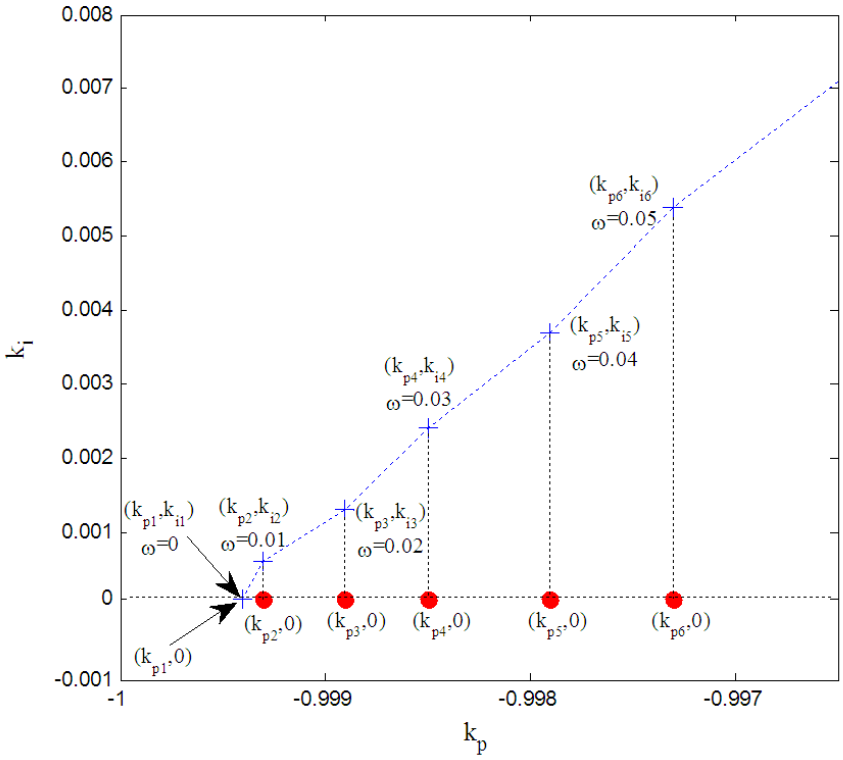

FIGURE 5. The coordinates of (k_p, k_i) points constituting the stability boundary locus and their projections for the real root boundary line for $\omega \in [0, 0.05]$

as follows

$$k_{pw} = \frac{1}{n}\sum_{j=1}^{n} k_{pj}, \tag{22}$$

$$k_{iw} = \frac{1}{2 \cdot n}\sum_{j=1}^{n} k_{ij}. \tag{23}$$

Thus, the weighted geometrical center using (22) and (23) can be found precisely. It is clear that smaller step size of ω provides greater accuracy.

Reconsider the FOPTD system given in Example 2.1. When the weighted geometrical center of the stability region in Figure 3 is computed by using (22) and (23), the PI controller parameters are obtained as $k_p = 1.0549$ and $k_i = 1.1811$. In Figure 6, weighted geometrical center of the FOPTD system is given.

4. **Simulations.** For the wisdom of the weighted geometrical center point is explained, a circular testing area centered at the weighted geometrical center point in the stability region is used for the simulations. The testing area is shown in Figure 7(a). Diameter of the testing area centered at weighted geometrical center point (|AB|) is one unit. The controllers used in simulations are computed by dividing the line segment |AB| into ten equal parts according to angle Θ which is the angle between |AB| and horizontal axis. Thus, sixty-six controllers are obtained by using six different values of angle Θ (0°, 30°, 60°, 90°, 120° and 150°) for the simulations. The controllers on |AB| are named as C_1, C_2, ..., C_{11} and showed in Figure 7(b). Control parameters of these controllers are given in Table 1. As for this, the controller on the weighted geometrical center is C_6.

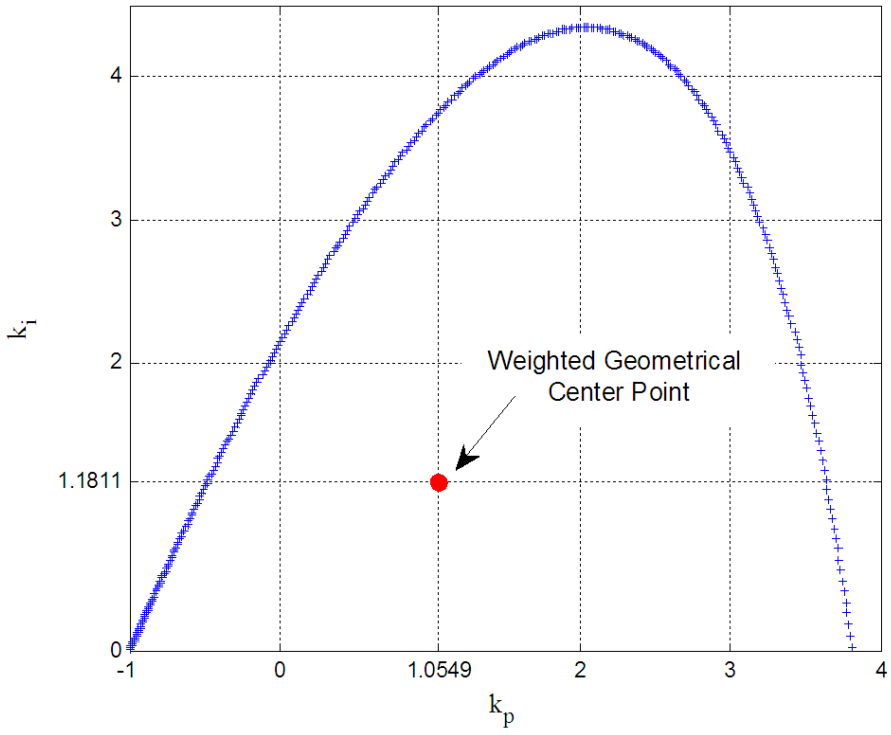

FIGURE 6. Weighted geometrical center of the system

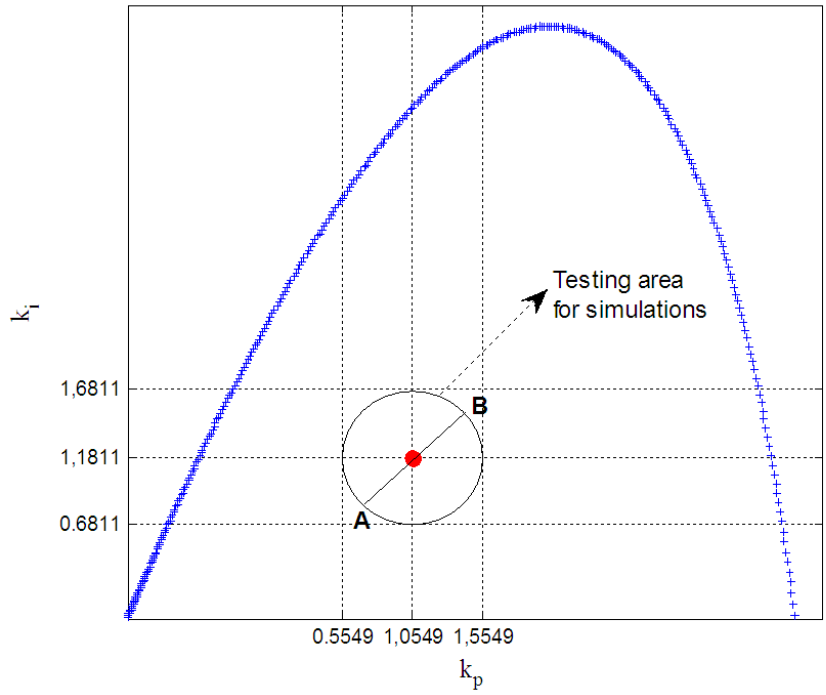

(a)

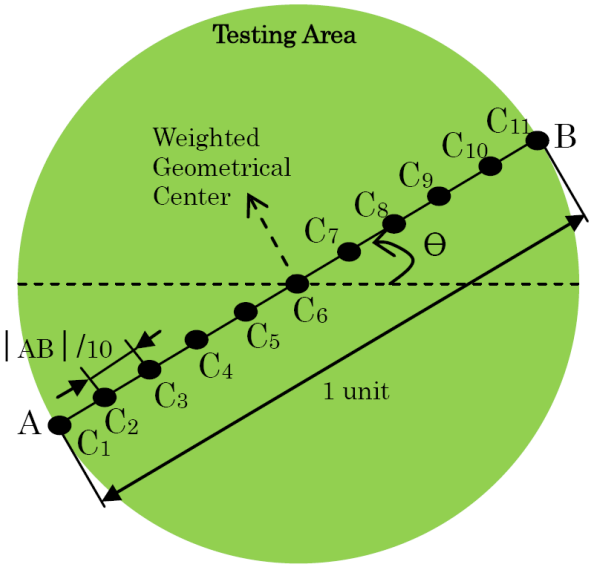

(b)

FIGURE 7. (a) Testing area around the weighted geometrical center for simulations and (b) zoomed testing area

The closed loop step responses are illustrated in Figures 8-13, for the controllers given in Table 1. The aims of the controllers minimize the transient state response performances. The performances are rise time, settling time and overshoot. Numerical values of these performances of the closed loops are given in Table 2 for comparison.

It can be seen from Figures 8-13 and Table 2 that when the controllers are changed from C_1 to C_{11} for all values of angle Θ, controller C_6 provides a good compromise between the rise time, settling time and overshoot performances. Since this result is illustrated

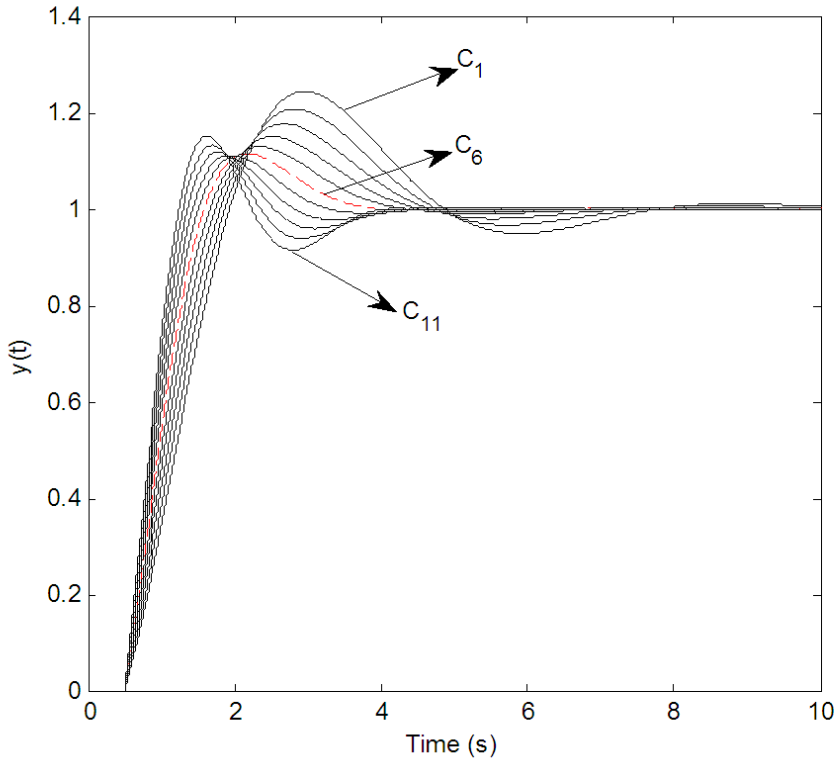

FIGURE 8. Step responses of the closed loops for $\Theta = 0°$

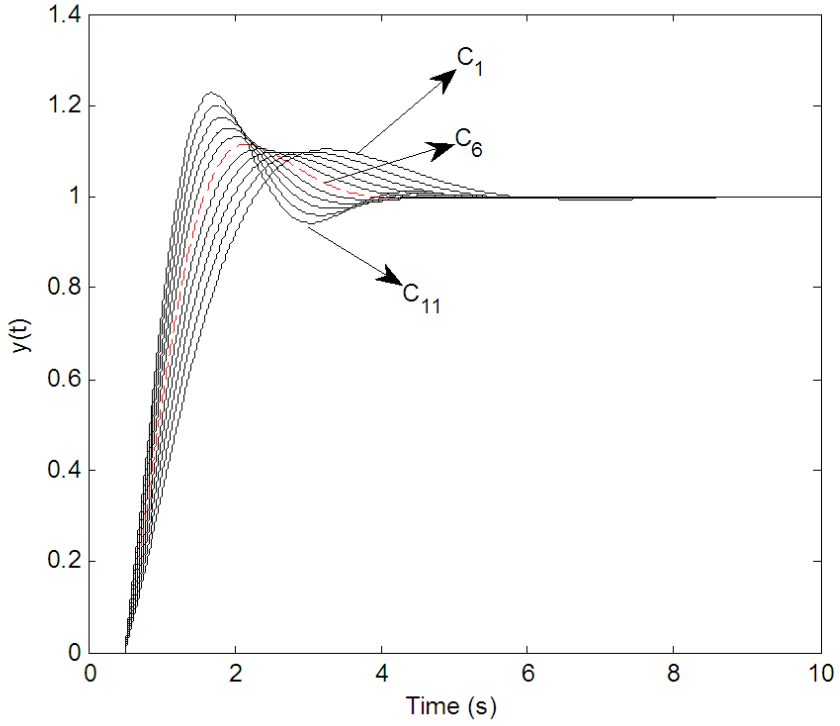

FIGURE 9. Step responses of the closed loops for $\Theta = 30°$

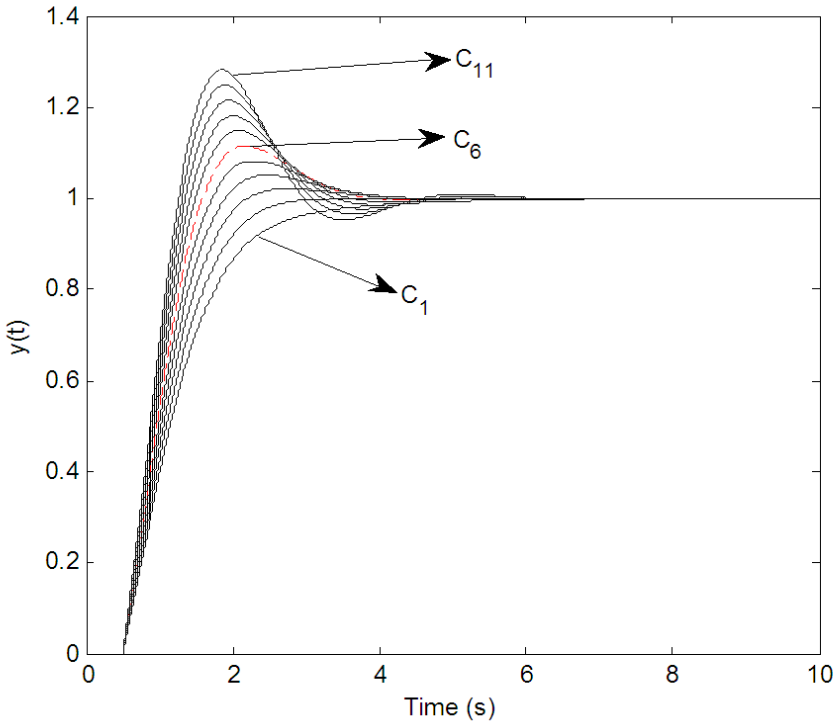

FIGURE 10. Step responses of the closed loops for $\Theta = 60°$

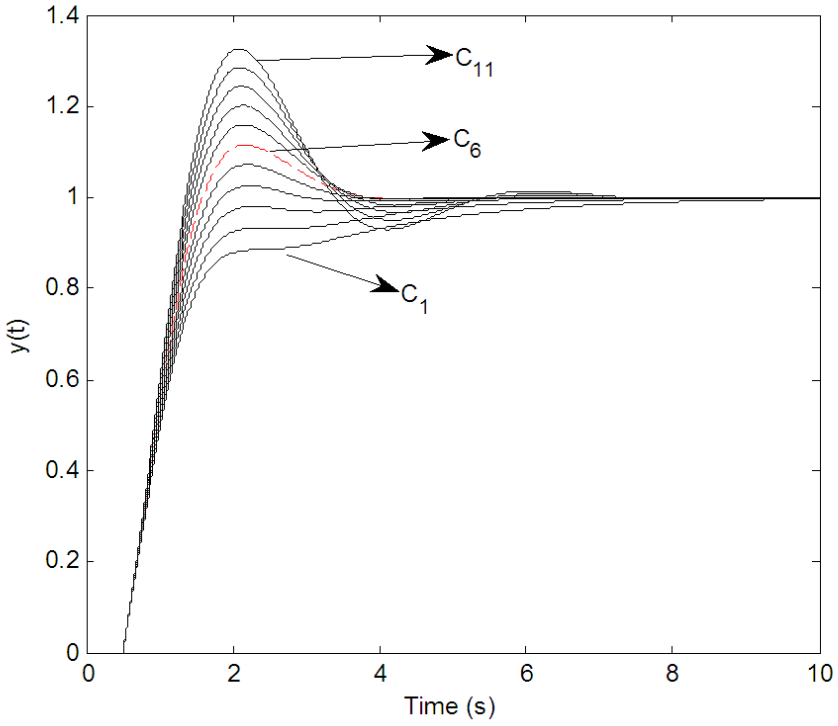

FIGURE 11. Step responses of the closed loops for $\Theta = 90°$

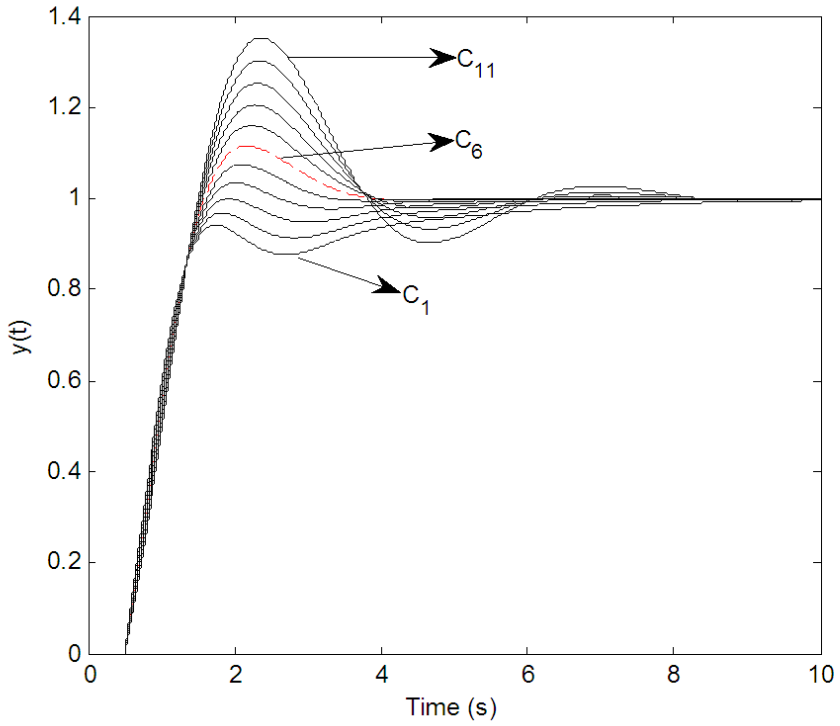

FIGURE 12. Step responses of the closed loops for $\Theta = 120°$

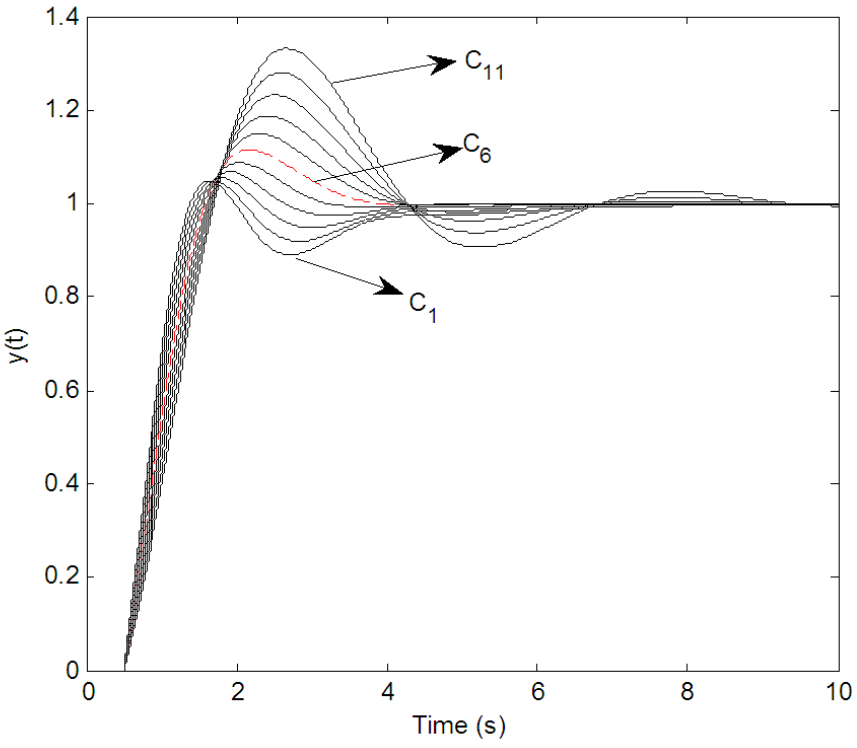

FIGURE 13. Step responses of the closed loops for $\Theta = 150°$

TABLE 1. Control parameters of the controllers used in simulations

		k_p	k_i			k_p	k_i
$\Theta = 0°$	C_1	0.5549	1.1811	$\Theta = 90°$	C_1	1.0549	0.6811
	C_2	0.6549	1.1811		C_2	1.0549	0.7811
	C_3	0.7549	1.1811		C_3	1.0549	0.8811
	C_4	0.8549	1.1811		C_4	1.0549	0.9811
	C_5	0.9549	1.1811		C_5	1.0549	1.0811
	C_6	1.0549	1.1811		C_6	1.0549	1.1811
	C_7	1.1549	1.1811		C_7	1.0549	1.2811
	C_8	1.2549	1.1811		C_8	1.0549	1.3811
	C_9	1.3549	1.1811		C_9	1.0549	1.4811
	C_{10}	1.4549	1.1811		C_{10}	1.0549	1.5811
	C_{11}	1.5549	1.1811		C_{11}	1.0549	1.6811
$\Theta = 30°$	C_1	0.6219	0.9311	$\Theta = 120°$	C_1	1.3049	0.7481
	C_2	0.7085	0.9811		C_2	1.2549	0.8347
	C_3	0.7951	1.0311		C_3	1.2049	0.9213
	C_4	0.8817	1.0811		C_4	1.1549	1.0079
	C_5	0.9683	1.1311		C_5	1.1049	1.0945
	C_6	1.0549	1.1811		C_6	1.0549	1.1811
	C_7	1.1415	1.2311		C_7	1.0049	1.2677
	C_8	1.2281	1.2811		C_8	0.9549	1.3543
	C_9	1.3147	1.3311		C_9	0.9049	1.4409
	C_{10}	1.4013	1.3811		C_{10}	0.8549	1.5275
	C_{11}	1.4879	1.4311		C_{11}	0.8049	1.6141
$\Theta = 60°$	C_1	0.8049	0.8347	$\Theta = 150°$	C_1	1.4879	0.9311
	C_2	0.8549	0.9213		C_2	1.4013	0.9811
	C_3	0.9049	1.0079		C_3	1.3147	1.0311
	C_4	0.9549	1.0945		C_4	1.2281	1.0811
	C_5	1.0049	1.0945		C_5	1.1415	1.1311
	C_6	1.0549	1.1811		C_6	1.0549	1.1811
	C_7	1.1049	1.2677		C_7	0.9683	1.2311
	C_8	1.1549	1.3543		C_8	0.8817	1.2811
	C_9	1.2049	1.4409		C_9	0.7951	1.3311
	C_{10}	1.2549	1.5275		C_{10}	0.7085	1.3811
	C_{11}	1.3049	1.6141		C_{11}	0.6219	1.4311

better, dimensionless performance values of the controllers and maximum variation from each other of these performances are given in Figures 14-19. Dimensionless values of rise time, settling time and overshoot performances are obtained by dividing the results given in Table 2 for each performance to their maximum values respectively. Thus the values of the performances scale to range of $[0, 1]$.

From Figures 14-19, the following conclusions can be made. It can be clearly seen that the rise time, settling time and overshoot values for the controller C_6 are closely at their best values. Furthermore, one can say that the controller C_6 is a good trade off point for accounting to the transient response performances. For example, from Figure 16, it is clear that the gap between the maximum and minimum values of the performances for controller C_1 is big; however, C_6 reduces to the minimum.

For robustness test of the controller C_6 respect to variations of the system parameters, it is considered that variation range of the coefficients of $D(s)$ given in (19) is $\pm\%10$, where

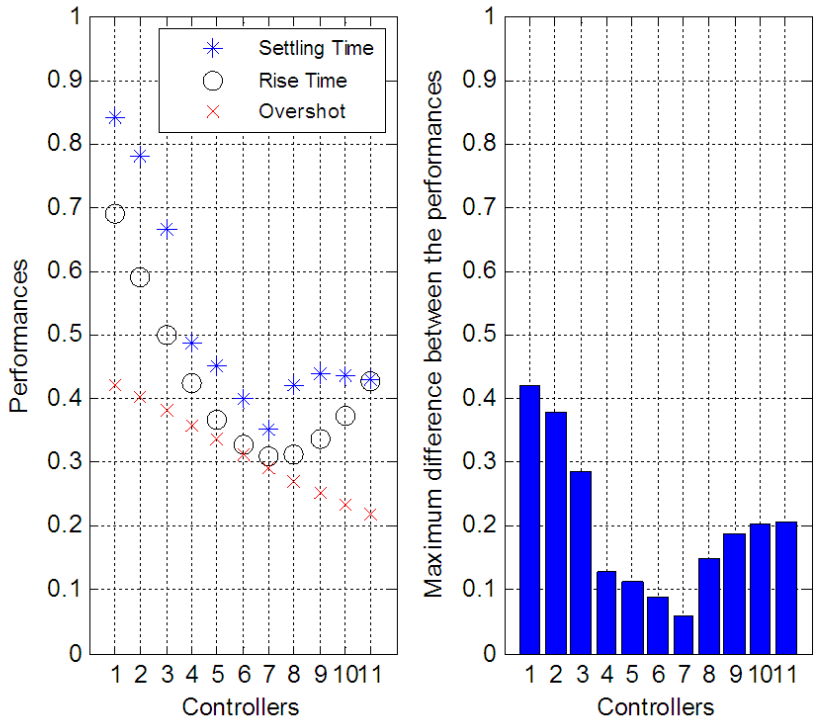

FIGURE 14. Performances of the controllers $\Theta = 0°$

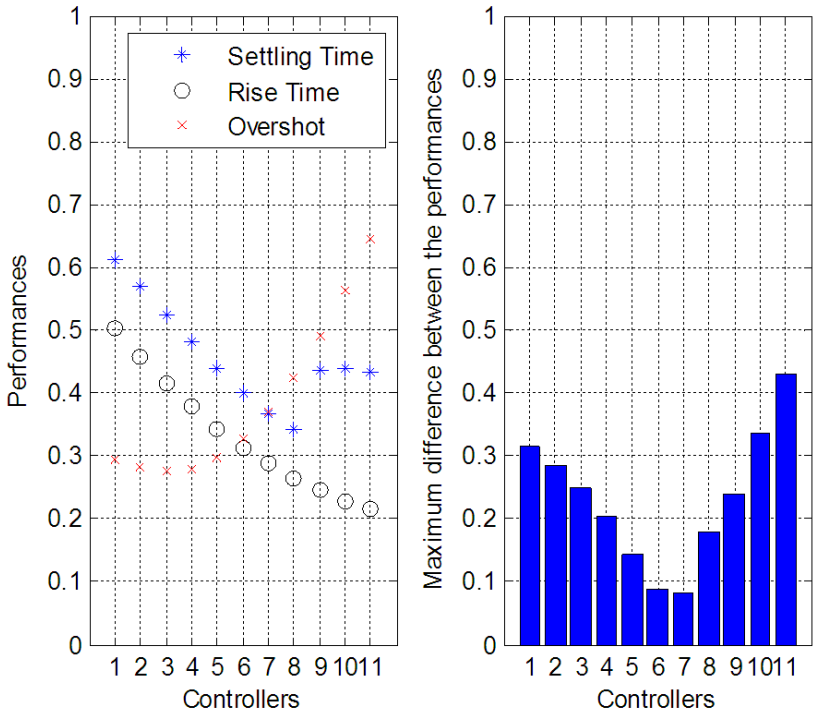

FIGURE 15. Performances of the controllers $\Theta = 30°$

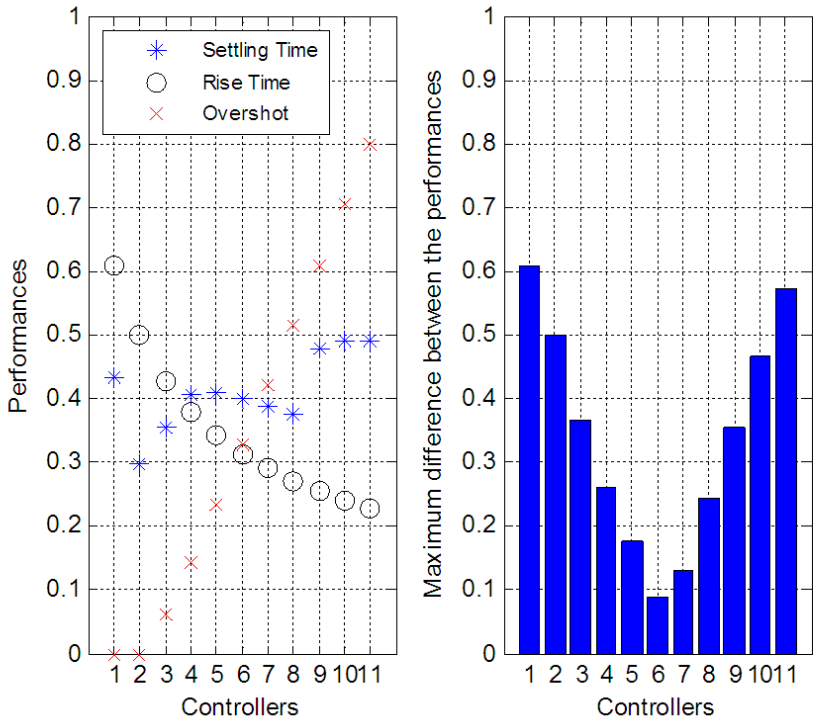

FIGURE 16. Performances of the controllers $\Theta = 60°$

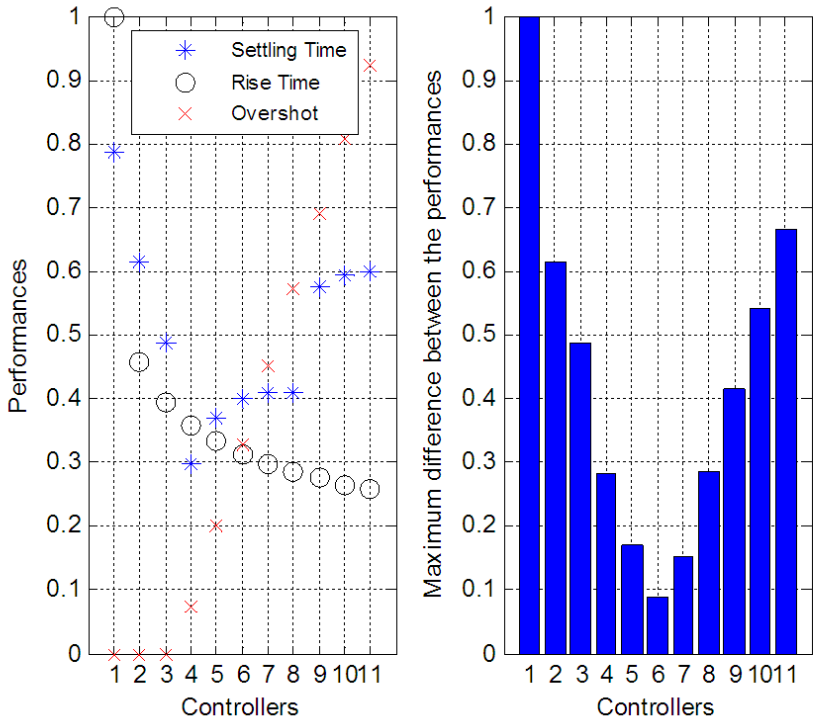

FIGURE 17. Performances of the controllers $\Theta = 90°$

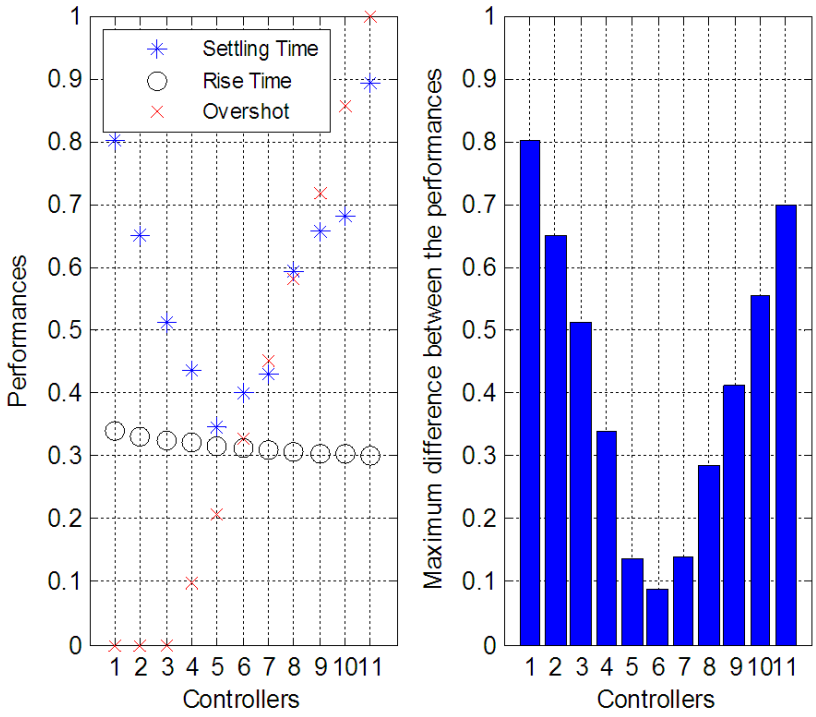

FIGURE 18. Performances of the controllers $\Theta = 120°$

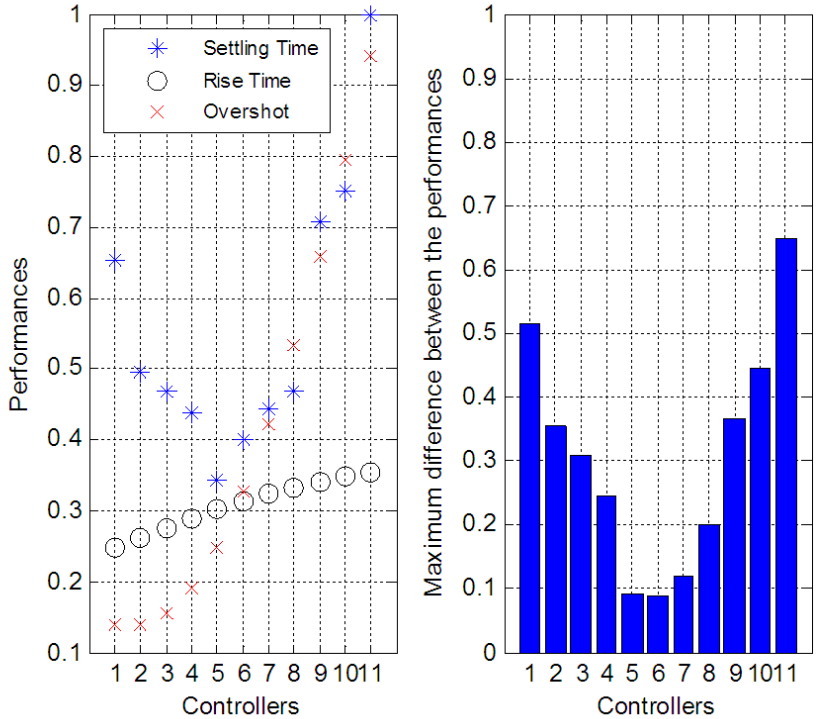

FIGURE 19. Performances of the controllers $\Theta = 150°$

TABLE 2. Numerical values of transient state performances of the controllers

		Rise Time (s)	Settling Time (s)	Overshot (%)			Rise Time (s)	Settling Time (s)	Overshot (%)
$\Theta = 0°$	C_1	1.0865	7.1155	24.3890	$\Theta = 90°$	C_1	2.5846	6.6477	0
	C_2	1.0391	6.6089	20.7785		C_2	1.1827	5.1936	0
	C_3	0.9861	5.6365	17.6438		C_3	1.0156	4.1186	0
	C_4	0.9291	4.1206	15.0021		C_4	0.9233	2.5037	2.5867
	C_5	0.8700	3.8030	12.9235		C_5	0.8596	3.1298	7.0941
	C_6	0.8110	3.3914	11.5223		C_6	0.8110	3.3914	11.5223
	C_7	0.7537	2.9662	10.8925		C_7	0.7717	3.4663	15.8777
	C_8	0.6999	3.5486	11.0296		C_8	0.7389	3.4572	20.1654
	C_9	0.6505	3.7124	11.8407		C_9	0.7109	4.8701	24.3852
	C_{10}	0.6059	3.6935	13.2106		C_{10}	0.6866	5.0214	28.5285
	C_{11}	0.5663	3.6304	15.0266		C_{11}	0.6653	5.0726	32.5781
$\Theta = 30°$	C_1	1.3031	5.1586	10.4360	$\Theta = 120°$	C_1	0.8748	6.7852	0
	C_2	1.1863	4.7992	9.9632		C_2	0.8555	5.5057	0
	C_3	1.0772	4.4397	9.7522		C_3	0.8411	4.3253	0
	C_4	0.9775	4.0788	9.8875		C_4	0.8295	3.6896	3.4298
	C_5	0.8886	3.7227	10.4603		C_5	0.8196	2.9275	7.3300
	C_6	0.8110	3.3914	11.5223		C_6	0.8110	3.3914	11.5223
	C_7	0.7437	3.1099	13.0626		C_7	0.8030	3.6271	15.9419
	C_8	0.6856	2.8869	15.0224		C_8	0.7955	5.0060	20.5462
	C_9	0.6354	3.6978	17.3266		C_9	0.7884	5.5387	25.3102
	C_{10}	0.5921	3.7062	19.9104		C_{10}	0.7814	5.7480	30.2202
	C_{11}	0.5546	3.6551	22.7205		C_{11}	0.7744	7.5356	35.2686
$\Theta = 60°$	C_1	1.5725	3.6611	0	$\Theta = 150°$	C_1	0.6448	5.5182	4.8768
	C_2	1.2918	2.5044	0		C_2	0.6792	4.1756	4.9130
	C_3	1.1097	2.9957	2.1879		C_3	0.7139	3.9484	5.5141
	C_4	0.9814	3.4348	5.1180		C_4	0.7480	3.7008	6.7816
	C_5	0.8856	3.4627	8.2666		C_5	0.7806	2.8909	8.7840
	C_6	0.8110	3.3914	11.5223		C_6	0.8110	3.3914	11.5223
	C_7	0.7505	3.2870	14.8352		C_7	0.8384	3.7509	14.9110
	C_8	0.7003	3.1756	18.1785		C_8	0.8626	3.9486	18.8377
	C_9	0.6578	4.0589	21.5361		C_9	0.8832	5.9754	23.2231
	C_{10}	0.6212	4.1588	24.8983		C_{10}	0.9001	6.3389	28.0301
	C_{11}	0.5895	4.1593	28.2593		C_{11}	0.9131	8.4470	33.2506

$D(s)$ is the characteristic equation of the plant. Accordingly, Kharitonov polynomials of $D(s)$ are given in (24)-(27).

$$D_1(s) = 0.9 \cdot s + 0.9 \tag{24}$$

$$D_2(s) = 1.1 \cdot s + 1.1 \tag{25}$$

$$D_3(s) = 0.9 \cdot s + 1.1 \tag{26}$$

$$D_4(s) = 1.1 \cdot s + 0.9 \tag{27}$$

Step responses of the controller C_6 for Kharitonov polynomials of $D(s)$ are given in Figure 20, where it is seen that controller C_6 exhibits a good robust performance in spite of variations of the system parameters.

5. **Conclusions.** A new concept for the PI control of time delay systems is presented in this paper. The concept is weighted geometrical center point of the stability region of the PI control system in the control parameters plane. The controller on the weighted geometrical center and its adjacent controllers are simulated. Simulation results show that the weighted geometrical center is a special point in terms of offering a good compromise

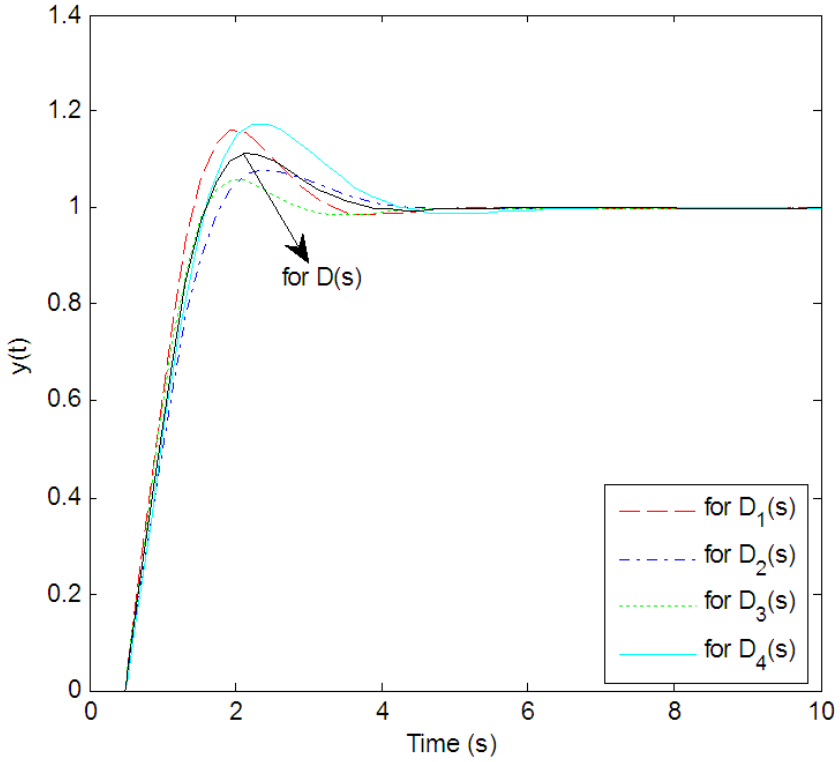

FIGURE 20. Performances of the controller C_6 respect to parameter uncertainties

between the rise-time, settling time and overshot performances. In future studies on this topic, seeking techniques based on the weighted geometrical center can be developed.

REFERENCES

[1] S. E. Hamamci, A robust polynomial-based control for stable processes with time delay, *Electrical Engineering*, vol.87, no.3, pp.163-172, 2005.

[2] T. Hagiwara, K. Yamada, I. Murakami, Y. Ando and T. Sakanushi, A design method for robust stabilizing modified PID controllers for time-delay plants with uncertainty, *International Journal of Innovative Computing, Information and Control*, vol.5, no.10(B), pp.3553-3563, 2009.

[3] J. P. Richard, Time-delay systems: An overview of some recent advances and open problems, *Automatica*, vol.39, no.10, pp.1667-1694, 2003.

[4] K. J. Astrom and T. Hagglund, The future of PID control, *Control Engineering Practice*, vol.9, pp.1163-1175, 2001.

[5] M. Zhuang and D. P. Atherton, Automatic tuning of optimum PID controllers, *IEE Proc. of D*, vol.140, no.3, pp.216-224, 1993.

[6] K. J. Astrom and T. Hagglund, PID controllers: Theory, design and tuning, *Instrument Society of America*, Nort Carolina, 1995.

[7] M. T. Ho, A. Datta and S. P. Bhattacharyya, A new approach to feedback stabilization, *Proc. of the 35th CDC*, pp.4643-4648, 1996.

[8] M. T. Ho, A. Datta and S. P. Bhattacharyya, A linear programming characterization of all stabilizing PID controllers, *Proc. of Amer. Contr. Conf.*, 1997.

[9] M. T. Ho, A. Datta and S. P. Bhattacharyya, A new approach to feedback design part I: Generalized interlacing and proportional control, *Tech. Report TAMU-ECEP7-001-A*, Dept. of Electrical Eng., Texas A&M Univ., College Station, TX, 1997.

[10] M. T. Ho, A. Datta and S. P. Bhattacharyya, A new approach to feedback design pan II: PI and PID controllers, *Tech. Report TAMU ECE97-0OI-B*, Dept. of Electrical Eng., Texas A&M Univ., College Station, TX, 1997.

[11] N. Munro and M. T. Soylemez, Fast calculation of stabilizing PID controllers for uncertain parameter systems, *Proc. of Symposium on Robust Control*, Prague, 2000.
[12] M. T. Soylemez, N. Munro and H. Baki, Fast calculation of stabilizing PID controllers, *Automatica*, vol.39, pp.121-126, 2003.
[13] N. Tan and D. P. Atherton, Feedback stabilization using the Hermite-Biehler theorem, *International Con. on the Control of Industrial Processes*, Newcastle, UK, 1999.
[14] J. Ackermann and D. Kaesbauer, Design of robust PID controllers, *European Control Conference*, pp.522-527, 2001.
[15] Z. Shatiei and A. T. Shenton, Frequency domain design of PID controllers for stable and unstable systems with time delay, *Auromotica*, vol.33, pp.2223-2232, 1997.
[16] Y. J. Huang and Y. J. Wang, Robust PID tuning strategy for uncertain plants based on the Kharitonov theorem, *ISA Transactions*, vol.39, pp.419-431, 2000.
[17] N. Tan, I. Kaya and D. P. Atherton, Computation of stabilizing PI and PID controllers, *IEEE Conference on Control Applications*, Istanbul, Turkey, 2003.
[18] Y. J. Wang, Graphical computation of gain and phase margin specifications-oriented robust PID controllers for uncertain systems with time-varying delay, *Journal of Process Control*, vol.21, pp.475-488, 2011.
[19] C. Onat, S. E. Hamamci and S. Obuz, A practical PI tuning approach for time delay systems, *IFAC*, Boston, USA, 2012.
[20] S. R. Padma, M. N. Srinivas and M. Chidambaram, A simple method of tuning PID controllers for stable and unstable FOPTD systems, *Computers and Chemical Engineering*, vol.28, pp.2201-2218, 2004.
[21] S. Majhi, On-line PI control of stable processes, *Journal of Process Control*, vol.15, pp.859-867, 2005.